Acta Pharmaceutica Sinica B 2022;12(2):747−758

Chinese Pharmaceutical Association
Institute of Materia Medica, Chinese Academy of Medical Sciences

Acta Pharmaceutica Sinica B

www.elsevier.com/locate/apsb
www.sciencedirect.com

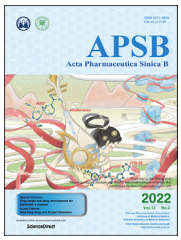

ORIGINAL ARTICLE

Ample dietary fat reduced the risk of primary vesical calculi by inducing macrophages to engulf budding crystals in mice

Huiling Chen[a,†], Kaiqiang Hu[a,†], Yaru Liang[a], Yuqi Gao[a], Chenye Zeng[a], Kang Xu[a], Xiaojin Shi[a], Liyuan Li[a], Yuemiao Yin[a], Yi Qiao[b], Ying Qiu[c], Qingfei Liu[a], Zhao Wang[a,*]

[a]*School of Pharmaceutical Sciences, Tsinghua University, Beijing 100084, China*
[b]*Urology Department, Peking Union Medical College Hospital, Beijing 100730, China*
[c]*School of Medicine, Tsinghua University, Beijing 100084, China*

Received 24 March 2021; received in revised form 11 May 2021; accepted 9 July 2021

KEY WORDS

Primary vesical calculi;
Diet;
High-fat;
D,L-Choline tartrate;
Macrophage;
CXCL14;
Fatty acid;
Urothelium

Abstract Although primary vesical calculi is an ancient disease, the mechanism of calculi formation remains unclear. In this study, we established a novel primary vesical calculi model with D,L-choline tartrate in mice. Compared with commonly used melamine and ethylene glycol models, our model was the only approach that induced vesical calculi without causing kidney injury. Previous studies suggest that proteins in the daily diet are the main contributors to the prevention of vesical calculi, yet the effect of fat is overlooked. To assay the relationship of dietary fat with the formation of primary vesical calculi, D,L-choline tartrate-treated mice were fed a high-fat, low-fat, or normal-fat diet. Genetic changes in the mouse bladder were detected with transcriptome analysis. A high-fat diet remarkably reduced the morbidity of primary vesical calculi. Higher fatty acid levels in serum and urine were observed in the high-fat diet group, and more intact epithelia in bladder were observed in the same group compared with the normal- and low-fat diet groups, suggesting the protective effect of fatty acids on bladder epithelia to maintain its normal histological structure. Transcriptome analysis revealed that the macrophage differentiation-related gene C−X−C motif chemokine ligand 14 (*Cxcl14*) was upregulated in the bladders of high-fat diet-fed mice compared with those of normal- or low-fat diet-fed mice, which was consistent with histological observations. The expression of CXCL14 significantly increased in the bladder in the high-fat diet group. CXCL14 enhanced the recruitment of macrophages to the crystal nucleus and induced the transformation of M2 macrophages, which led to phagocytosis of budding crystals and

*Corresponding author. Tel./fax: +86 10 62772241.
E-mail address: zwang@tsinghua.edu.cn (Zhao Wang).
[†]These authors made equal contributions to this work.
Peer review under responsibility of Chinese Pharmaceutical Association and Institute of Materia Medica, Chinese Academy of Medical Sciences.

https://doi.org/10.1016/j.apsb.2021.08.001

prevented accumulation of calculi. In human bladder epithelia (HCV-29) cells, high fatty acid supplementation significantly increased the expression of CXCL14. Dietary fat is essential for the maintenance of physiological functions of the bladder and for the prevention of primary vesical calculi, which provides new ideas for the reduction of morbidity of primary vesical calculi.

1. Introduction

In contrast to secondary vesical calculi, primary vesical calculi are formed in the bladder under the condition of a normal upper urinary tract. It was reported that primary vesical calculi mainly occurred in children with malnutrition[1]. It has been shown that the absence of breastfeeding or animal dairy products is responsible for the occurrence of primary vesical calculi, but the mechanism remains unclear[2]. Previous studies suggest that the proteins in milk contribute most to the prevention of vesical calculi[1], yet the effect of fat in milk has been overlooked. The goal of this study was to evaluate the effect of dietary fat on the formation of primary vesical calculi and explore the molecular mechanism, which is expected to enhance our understanding of the pathophysiological mechanisms of this disease and provide novel therapeutic approaches against malnourishment-related diseases.

A major constraint of the investigation of primary vesical calculi is modeling, as the pathogenesis of this condition is not fully understood. At present, the methods commonly used to establish vesical calculi models, including feeding rodents melamine[3,4], ethylene glycol[5,6] or terephthalic acid[7,8], have one major defect. The principle of these methods is to induce a large number of crystals in the urinary tracts of model animals in a short time. Instead of inducing primary vesical calculi, these methods normally induce renal trauma or renal calculi first[9,10]. D,L-Tartaric acids are legal food additives worldwide[11]. Previous studies observed that D,L-choline tartrate caused stones as D,L-calcium tartrate is insoluble in water, but the mechanism was not intensively studied[12,13]. Based on this, we established a novel primary vesical calculus mouse model using D,L-choline tartrate. Our model does not cause renal injury, which has an obvious advantage for investigating the mechanism of vesical calculi formation.

Macrophages play a critical role in the pathogenesis of urolithiasis. Macrophage migration occurs in the crystal-forming region at an early stage[14], and crystal phagocytosis by macrophages prevents the crystal nucleus from developing into calculus[15]. Some investigators have reported that macrophages aggravate renal crystal formation in high-fat diet-fed mice by promoting inflammatory reactions[16]. However, whether dietary fat could activate macrophages in the urinary bladder, enhance the ability to eliminate pathogenic crystals, and therefore protect the bladder from calculi remains to be proven. In this paper, to investigate how dietary fat affects calculi formation, D,L-choline tartrate-induced model mice were treated with a high-, normal-, or low-fat diet. These results showed that high-fat content in the diet remarkably reduced the morbidity of primary vesical calculi. Transcriptome analysis revealed that macrophages were more active in the bladders of mice fed a high-fat diet than in those of mice fed a normal- or low-fat diet, which was also confirmed by histological tests. In addition, different concentrations of fatty acids were added to the human bladder epithelia (HCV-29) cell medium *in vitro* for molecular mechanism verification. Taken together, the results from our study suggested that dietary fat was essential for the prevention of primary vesical calculi.

2. Materials and methods

2.1. Chemical and biological reagents

Melamine [2,4,6-triamino-*s*-triazine, CAS No. 108-78-1] was purchased from Tokyo Chemical Industry Co., Ltd. (Shanghai, China). Choline chloride was purchased from Jinan Asia Pharmaceutical Co., Ltd. (Jinan, China). Ethylene Glycol was purchased from Beijing Tongguang Fine Chemical Co., Ltd. (Beijing, China). C−X−C motif chemokine ligand 14 (CXCL14) antibody, F4/80 antibody and glyceraldehyde-3-phosphate dehydrogenase (GAPDH) antibody were purchased from Cell Signaling Technology (Danvers, MA, USA). All other chemicals were of analytical grade and used as received.

2.2. Animals and diets

Four-week-old male C57BL/6J mice were purchased from the Laboratory Animal Research Center of Tsinghua University (Beijing, China). All mice were housed in a temperature-controlled environment at 22 ± 2 °C with 12-h light/dark cycles. All applicable institutional and/or national guidelines for the care and use of animals were followed. All protocols were approved by the Institutional Animal Care and Use Committee of China (Beijing, China). The animal protocol serial number for the animal experiments was 14-WZ1.

All mice were labelled and weighed before the experiment started and then randomly assigned to three groups using random number table method. A standard AIN-93G diet containing D,L-choline tartrate was chosen as the basic food. To choose the most appropriate primary vesical calculus mouse model, after 1-week acclimation, mice were assigned to the following groups: (1) the D,L-choline tartrate-treated group, in which mice were fed the AIN-93G diet containing D,L-choline tartrate and given free access to water with 4-week or 20-week intervention; (2) the melamine-treated group, in which mice were fed the AIN-93G diet containing 9397 ppm melamine and given free access to water with 2-week intervention; and (3) the ethylene glycol-treated group, in which mice were fed the AIN-93G diet containing choline chloride and given free access to water with 1% ethylene glycol accompanied by administration of 1,25-$(OH)_2$-VitD_3 (Aladdin Chemistry, Shanghai, China) every other day with 4-week intervention.

2.3. Study design

To investigate the effect of dietary fat on the formation of primary vesical calculi, after 1 week of acclimation, mice were assigned to 3 groups: the high-fat (HF), normal-fat (NF) or low-fat (LF) groups. All food ingredients were based on the standard AIN-93G diet. Mice in the NF group were fed the standard AIN-93G diet (64% carbohydrate, 19% protein, and 17% fat in calories). The high-fat diet (30% carbohydrate, 19% protein, and 51% fat in calories) and the low-fat diet (75.4% carbohydrate, 19% protein, and 5.6% fat in calories) were fed to the mice in the HF and LF groups, respectively. The carbohydrates in the diets were composed of starch, maltodextrin and sucrose; the protein was composed of casein and cystine; and the fat was composed of soybean oil and lard. The energy factor of protein and carbohydrates was calculated based on 4 kcal/g. The energy factor of fat was calculated based on 9 kcal/g. In addition to essential vitamins, minerals and antioxidants, the same quality of D,L-choline tartrate (2.5 g/kg) was added to the diets as a calculi inducer. To ensure that each group of mice consumed the same amount of D,L-calcium tartrate, all groups were provided with the same quality of food according to how much the HF group mice consumed during the acclimation period. All mice in the HF, NF and LF groups were given free access to water. These mice were fed for 4 or 20 weeks of dietary intervention. Body weight and drinking water intake (volume) were monitored once a week. The daily urine volume of each mouse was monitored after a 4-week dietary intervention.

The HCV-29 cell lines were purchased from Tongpai Biotechnology Co., Ltd. (Shanghai, China), and these cells were maintained in DMEM (Corning Science) containing 10% fetal bovine serum (Coring Science) and 1% penicillin/streptomycin (Coring Science) to verify the molecular mechanism. HCV-29 cells were incubated at 37 °C with 5% CO_2 until they reached 60% confluence. The cells were treated with a mixture of 200 μmol/L palmitic acid (Aladdin Chemistry) and 100 μmol/L oleic acid (Aladdin Chemistry) or a mixture of 400 μmol/L palmitic acid and 200 μmol/L oleic acid for 24 h. Then, the supernatant was collected for enzyme-linked immunosorbent assay. Adherent HCV-29 cells were treated with 0.25% trypsin (Coring Chemistry) for 5 min and then harvested for RT-qPCR and Western blotting detection.

2.4. Sample collection

Mice were anaesthetized with an overdose of pentobarbital, and bladder and bladder calculi were removed for further investigation. First, we exposed the bladder, peeled the fatty tissue around the bladder with forceps, and then removed the bladder with surgical scissors. Next, we opened the bladder from the middle part and collected all calculi in the bladder. Note that the bladder stayed flat throughout the process, and as many calculi as possible were collected. These bladder samples were fixed with 4% formaldehyde and then prepared for routine staining. The bladder samples stored at −80 °C were used for protein content analysis, RNA sequencing and/or real-time quantitative PCR analysis.

Serum was collected by heart punctures before the mice were sacrificed, and these samples were stored at −80 °C to measure the calcium concentration and tartaric acid concentration. Fresh voided urine collection was performed at 4 time points (around 6:00, 12:00, 18:00 and 24:00) in one day with different four weeks of dietary intervention. The mice were placed on a clean grid, under which a clean tray was used to collect urine. The mice could drink and eat freely on the grid until they had excreted urine. Urine was collected within 5 min of excretion, and the pH values were measured with a MicropH Meter (Mettler-Toledo).

2.5. Chemical composition analysis

Before chemical composition analysis, the bladder calculi were washed with distilled water and dried in an oven at 100 °C overnight. For Fourier Transform Infrared Spectroscopy (FTIR) analysis, the dried samples were first ground to powder with a drying mortar. Then, 1 mg of calculi powder and 200 mg of predried pure potassium bromide powder were mixed with a press machine. When pressing, the pressure gauge had a gravity of 20 mkp until a translucent sheet was formed, and then the sample was quickly placed in an infrared spectrum tank for scanning. FTIR spectra were recorded by using a Tensor-27 (Bruker, USA) spectrometer at a resolution of 2 cm^{-1}, and 32 scans were signal-averaged. The testing range was from 400 to 4000 cm^{-1}. The computer-generated spectra and composition were calculated automatically.

The ^{13}C solid nuclear magnetic resonance (NMR) spectra were recorded on a nuclear magnetic resonance spectrometer from Japan Electronics Co., Ltd. (JNM-ECA600, Tokyo, Japan) operating at 25 °C and 162 MHz for ^{13}C analysis. The 16 k-point spectra were acquired with 16 K points, a recycle delay of 5 s, a scan number of 5000, an acquisition time of 25 ms, and a ^{13}C 90° pulse. The ^{13}C 90° pulse length was 16 μs with an attenuation level of 3.3 dB.

2.6. Biochemical analysis

The concentrations of tartaric acid in serum and urine samples were analyzed with the metabolomics platform at Tsinghua University (Beijing, China). For derivatization, 40 μL of the supernatant (serum and urine) was mixed with 20 μL of 200 mmol/L 3-nitropheylhydrazine (J&K Scientific) in 50% aqueous acetonitrile (Macklin) and 20 μL of 120 mmol/L *N*-(3-dimethylaminopropyl)-NO-ethylcarbodiimide pyridine solution (Sigma−Aldrich) in the same solvent. The mixture was reacted at 40 °C for 30 min. After the reaction, this solution was dried by a SpeedVac (Thermo Fisher Scientific) and stored in a −80 °C freezer.

The concentrations of calcium in serum and urine samples were analyzed using a Calcium Colorimetric Assay Kit (BioVision, San Francisco, USA) following the manufacturer's instructions. The fatty acid levels in serum and urine were analyzed using a Free Fatty Acid Assay Kit (ab65341) purchased from AmyJet Scientific Inc. (Wuhan, China), following the manufacturer's instructions. The pH values of urine samples were analyzed by using a pH meter [FE28-Micro, Mettler-Toledo International Trading (Shanghai) Co., Ltd.] following the manufacturer's instructions.

2.7. Real-time quantitative PCR analysis

For real-time quantitative PCR analysis, total mRNA of bladder tissues after 4 weeks of different dietary intervention and harvested HCV-29 cells were extracted by TRIzol (Thermo Fisher Science). RNA concentrations and purity were estimated by determining the A260/A230 ratio with a NanoDrop 2000c (Thermo Fisher Scientific). cDNA was obtained by using a FastQuant RT Kit [Tiangen

Biotech (Beijing) Co., Ltd.)] and used for real-time PCR analysis with SuperReal PreMix Plus [Tiangen Biotech (Beijing) Co., Ltd.)] according to the 2-step reaction program. The primers used for the *Cxcl14* gene were as follows: Fw, 5′-TACCCACACTGCGAGGAGAAGA-3′; Rv, 5′-CGCTTCTCGTTCCAGGCATTGT-3′. The primers used for the *Gapdh* gene were as follows: Fw, 5′-CATGGCCTTCCGTGTTCCTA-3′; Rv, 5′- CCTGCTTCACCACCTTCTTGAT-3′.

2.8. Histological analysis

For pathological analysis, half of these bladder tissues were fixed with 4% formaldehyde and embedded in paraffin. Along the transverse section, the paraffin was cut into 4 μm slices and stained with a Hematoxylin-Eosin Staining Kit (Beyotime Biotechnology).

Masson's Trichrome Staining Kit (Solarbio Life Sciences) was used to observe collagen deposition areas. Under an optical microscope, the collagen fibers were blue, and the muscle fibers were red. The detailed experimental methods were performed according to previous literature[17].

Alizarin red staining was used to detect calcium deposition. The frozen sections were fixed in 95% ice-cold ethanol (Macklin) and then stained with 2% alizarin red purchased from Solarbio Life Sciences (Beijing, China) for 15 min at room temperature. The emergence of mineralized nodules was considered positive.

2.9. Immunological staining

The paraffin-embedded bladder tissues were cut into 4 μm sections for immunological analysis. For immunohistochemical staining, the sections were deparaffinated, hydrated and incubated with primary F4/80 antibodies at 4 °C overnight. After washing in Tris-HCl buffer (Beyotime Biotechnology) mixed with 0.1% Tween 20 (Beyotime Biotechnology), these sections were continually incubated with a secondary antibody labeled with hydrogen peroxide oxidoreductase. All these stains were visualized with an Olympus microscope (Tokyo, Japan). For immunofluorescence staining, after the sections were incubated with the primary F4/80 antibody at 4 °C overnight and the secondary antibodies for 1 h at room temperature; appropriate second primary antibodies (CD86, with dilution 1:80/CD163, dilution 1:100) were applied at 4 °C overnight, and the second secondary antibodies were applied for another 1 h at room temperature. Then, the sections were counterstained with 4,6-diamino-2-phenylindole. Images were collected with a Zeiss Axio Scan.Z1 scanner (Carl Zeiss, Jena, Germany).

2.10. Western blotting

For Western blotting, bladders and harvested HCV-29 cells were resuspended in lysis buffer. The proteins were extracted, and samples were resolved on a 10% sodium dodecyl sulfonate-polyacrylamide gel and then transferred to polyvinylidene fluoride membranes (Merck Millipore Ltd.). Antibodies against the following proteins were used: CXCL14 and GAPDH. Goat anti-rabbit immunoglobulin G was also used.

2.11. Statistical analysis

The results were presented as the mean ± standard error of mean (SEM). For the animal experiments, each group contained at least six mice. For the cell experiments, at least three independent experiments were conducted. Data were analyzed with GraphPad Prism 5.0 software (GraphPad Software Inc., San Diego, CA, USA). One-way ANOVA test were used to analysis of three groups. Differences were considered significant when the P value < 0.05. To directly compare the differences among the groups, some data from the HF and LF groups were normalized to the NF group.

3. Results

3.1. Modeling primary vesical calculi with D,L-choline tartrate

To establish a urinary calculi mouse model, three calculi inducers, D,L-choline tartrate, melamine and ethylene glycol, were selected. According to the literature, the optimal induction time was chosen for different calculi inducers. These results show that mice in the D,L-choline tartrate-treated group (after 20 weeks of dietary intervention) and in the melamine-treated group (after 2 weeks of dietary intervention) demonstrated a large number of primary vesical calculi (Fig. 1A). No visible calculi were found in the bladders of mice in the other groups (Fig. 1A).

Hematoxylin and eosin (H&E) results reveal that the mucous layers of bladders were severely damaged in mice fed D,L-choline tartrate-supplemented food for 20 weeks and in mice fed melamine-supplemented food for 2 weeks (Fig. 1B). In particular, we found that the mouse bladder epithelia changed when D,L-choline tartrate-supplemented feed was served for 4 weeks, and the bladder epithelia were no longer smooth and showed "spiculation-like" changes. The "spiculation-like" changes of bladder epithelia in the ethylene glycol-treated group mice were more severe than those in the D,L-choline tartrate-treated group mice served for 4 weeks. Meanwhile, the mice in the ethylene glycol-treated and melamine-treated groups showed significant renal injury even before vesical calculi formed (Fig. 1C and D). However, the mice fed D,L-choline tartrate supplementation had no crystallization in the kidney and showed no renal injury (Fig. 1D and Supporting Information Fig. S1). These results suggest that D,L-choline tartrate is the best compound to induce a primary vesical calculus mouse model.

The characteristic absorption peaks of the calculi were obtained through spectrophotometry, which can be used to calculate the chemical composition. FTIR was selected to measure the primary vesical calculi composition of mice fed a D,L-choline tartrate diet after 20 weeks of intervention (Fig. 1E). These characteristic absorption peaks were found at 3478, 3368, 1599 and 630 ppm in the FTIR spectrum of vesical calculi. Previously, Kleinguetl et al.[13] reported a case of urolithiasis that might have been related to the use of drink supplements containing tartrate. The FTIR spectrum of vesical calculi was highly matched with the spectrum of the patient stone samples, and the composition was identified as calcium tartrate tetrahydrate. At the same time, the ^{13}C solid-state NMR results show that the carbon peak of vesical calculi was located at 75 and 180 ppm (Fig. 1F), which was consistent with calcium tartrate. From the above analysis, we confirmed that the chemical composition of primary vesical calculi induced by D,L-choline tartrate in our study was calcium tartrate tetrahydrate.

3.2. Dietary fat reduced the morbidity of primary vesical calculi

To evaluate the effect of dietary fat content on the formation of vesical calculi, mice in the HF, NF and LF groups were given a high-, normal-, or low-fat diet, respectively, for 20 weeks. Based

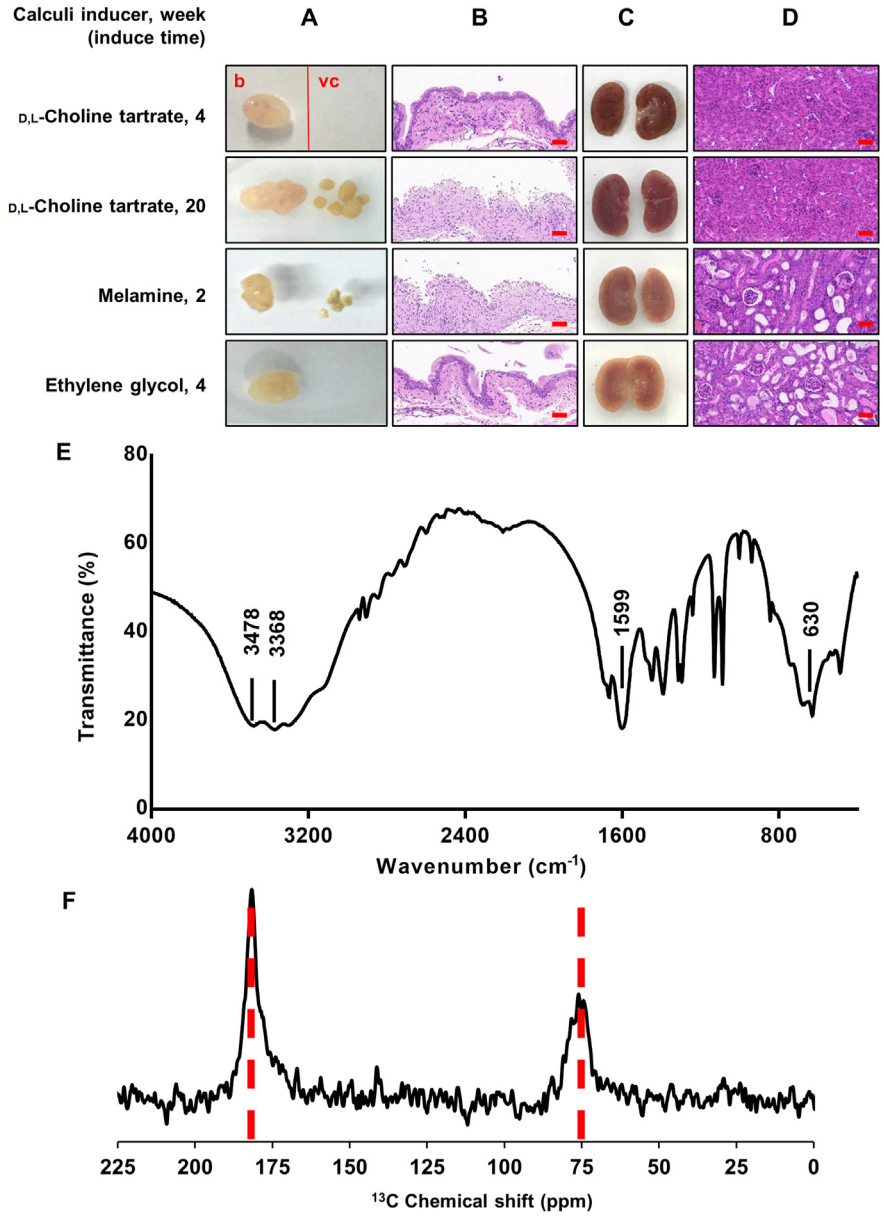

Figure 1 Establishment of a primary vesical calculus mouse model using D,L-choline tartrate. (A) Representative images of a bladder (left of the red line) and vesical calculi (right of the red line) after exposure to different calculi inducers. Obvious vesical calculi were found in the D,L-choline tartrate-treated and melamine-treated groups. (B) The bladders of mice were stained with Hematoxylin−Eosin (H&E) to visualize the structural differences among the different calculus inducer groups. (C) Representative images of kidneys after exposure to different calculi inducers. (D) The kidneys of mice were stained with H&E to visualize the structural differences among the different calculus inducer groups. (E) Fourier transform infrared (FTIR) analysis of vesical calculi. (F) ^{13}C solid nuclear magnetic resonance spectroscopy (NMR) spectrograph of vesical calculi. b, bladder; vc, vesical calculi. $n = 6$. Scale bar, 50 μm.

on appearance, the mice in the HF group were obviously fatter than those in the NF and LF groups as a result of the consumption of a high-fat diet (Fig. 2A). The mice in the LF group were slightly thinner than the mice in the NF group. The body weight of mice in the HF group continued to increase from 2 weeks until 20 weeks. With the extension of feeding time, the difference in body weight between the HF group and NF/LF groups became increasingly remarkable (Fig. 2B).

After 20 weeks of dietary intervention, the mice were sacrificed. No vesical calculi were observed in the HF group mouse bladders. Obvious vesical calculi were found in the NF and LF group mouse bladders (Fig. 2D−F). We also recorded the weight of bladders and vesical calculi in the different groups. We found that the weights of both the bladder (Fig. 2C) and the vesical calculi (Fig. 2E) in the HF group were significantly lower than those in the NF/LF groups. The above results suggest that a high-fat diet can reduce the morbidity of primary vesical calculi. We also measured the levels of total cholesterol, triglycerides, high-density lipoprotein cholesterol (HDL-C), and low-density lipoprotein cholesterol (LDL-C) in the serum of mice after 20 weeks of dietary intervention (Supporting Information Fig. S2). The total cholesterol in the serum of mice in the HF group was 2-fold higher

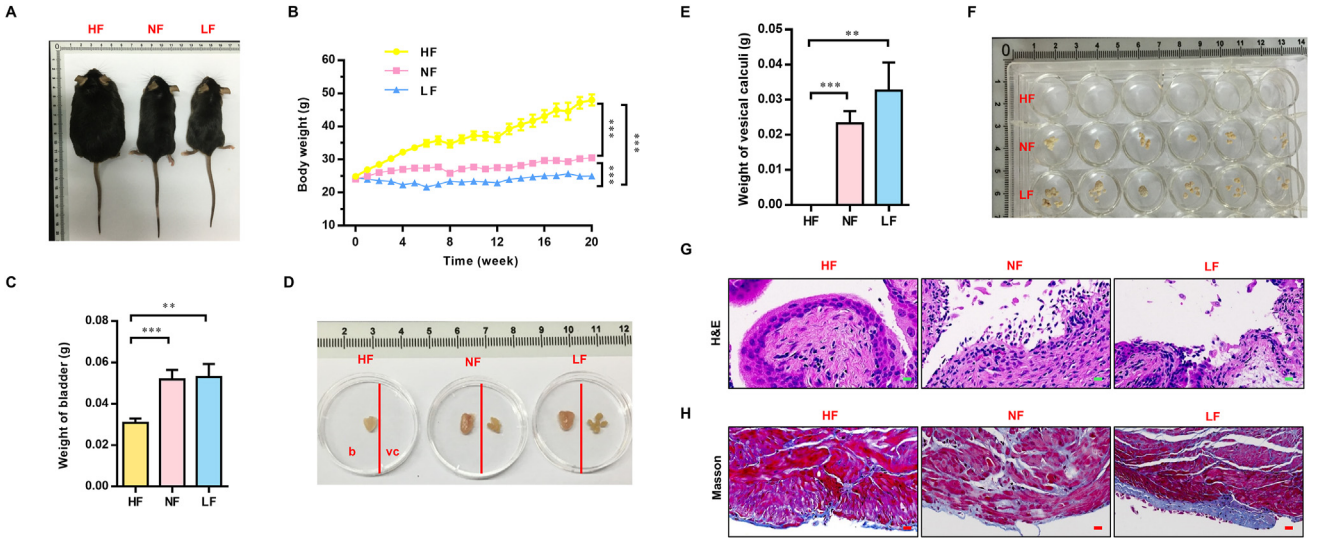

Figure 2 High-fat intake reduced the morbidity of vesical calculi after 20 weeks of dietary intervention. (A) Appearance of the mice in the different groups after 20 weeks of dietary intervention. (B) Changes in the body weight of mice. Body weight was measured every 7 days beginning in the acclimation period (7 days) and ending at 21 weeks. "0" represents the acclimation period. (C) Bladder weight of mice after 20 weeks of dietary intervention. (D) Representative images of the bladders (left of the red line) and vesical calculi (right of the red line) in the different groups after 20 weeks of dietary intervention. (E) Weight of the vesical calculi of mice after 20 weeks of dietary intervention. (F) Images of vesical calculi from each mouse in the different groups after 20 weeks of dietary intervention. Vesical calculi from each mouse were placed in each well of a 24-well plate. For histology, the bladder tissue of mice was stained with H&E (G) and Masson's Trichrome (H) to visualize the structural differences among different groups after 20 weeks of dietary intervention. HF, high-fat; NF, normal-fat; LF, low-fat. b, bladder; vc, vesical calculi. Data are presented as the mean ± SEM; $n = 6$. Significance was determined by the one-way ANOVA; $^{**}P < 0.01$, $^{***}P < 0.001$. Scale bar, 10 μm.

than that of mice in the NF group (Fig. S2A). No significant changes were found in serum triglycerides among the three groups (Fig. S2B). There was no dose-dependent relationship between the relative HDL-C and LDL-C levels and the diet in the three groups (Fig. S2C and S2D).

To explore the specific protective effects of a high-fat diet on the bladder, we performed H&E staining on bladders from different groups. These results revealed prominent microstructural differences in bladders between the HF group and NF/LF groups. The microstructure of the bladder urothelium from the NF and LF groups was severely damaged (Fig. 2G). However, the bladder urothelium remained normal in the HF group. Masson's trichrome staining showed that the degree of fibrosis in the muscular layers was significantly more severe in the NF and LF groups than in the HF group (Fig. 2H). We speculate that due to the existence of more vesical calculi in the NF and LF groups, the calculi might occasionally rub against the bladder urothelium, causing and accelerating the bladder fibrosis process in the NF and LF groups.

To determine the cause of primary vesical calculi, we must rule out the interference and damage of calculi on the bladder mucosal layer. We conducted an experiment to identify a time point before the formation of vesical calculi. Mice were sacrificed every 7 days to detect the time point. We found that the 4-week dietary intervention time was the time when no vesical calculi were formed. The basic animal parameters related to a 4-week dietary intervention with a high-, normal- or low-fat diet are shown in the supplemental materials (Supporting Information Fig. S3). We found that the body weights of mice in the HF group also changed significantly compared with those in mice of the NF and LF groups, even after 4 weeks of dietary intervention (Fig. S3A and S3D). There were no primary vesical calculi in any group, and the weight of the bladder was not different among these three groups (Fig. S3B and S3C). Moreover, there were no significant differences in the total cholesterol, triglyceride, HDL-C, and LDL-C in the serum of mice after 4 weeks of dietary intervention (Fig. S3E−S3H). However, the relative fatty acid levels in the serum and urine of mice were significantly higher in the HF group than in the NF/LF groups (Fig. 3A and B). As a result, the 4-week dietary intervention was regarded as a time point at which the high-fat diet had an effect but no vesical calculi formed.

Because the main composition of vesical calculi was calcium tartrate tetrahydrate, we further measured the concentration of calcium and tartaric acid in serum and urine after 4 weeks of dietary intervention. The results showed that among the high-, normal-, and low-fat diet groups, no significant differences in calcium and tartaric acid in serum or urine were observed (Fig. 3C−F). However, the volume of daily water intake and urine of mice in the LF group was significantly greater than that in the HF and NF groups (Fig. 3G and H). This finding was different from the clinical theory that high levels of water intake and urine volume accelerate the stone excretion process. The urine of mice fed different diets for four weeks was collected at 4 time points in one day, and the changes in urine pH value were detected. Compared with the NF and LF groups, the urine pH value of mice in the HF group was slightly lower at most points (Fig. 3I). In addition, no difference was observed in urinary sediment analysis of mice with 4-week different dietary intervention (Supporting Information Fig. S4). All the results of the 4-week dietary intervention revealed that although the physicochemical properties (pH value, water drinking and urine volume) did change before calculi formation in the bladder, that change was not responsible for the difference in calculi morbidity among these three groups. This

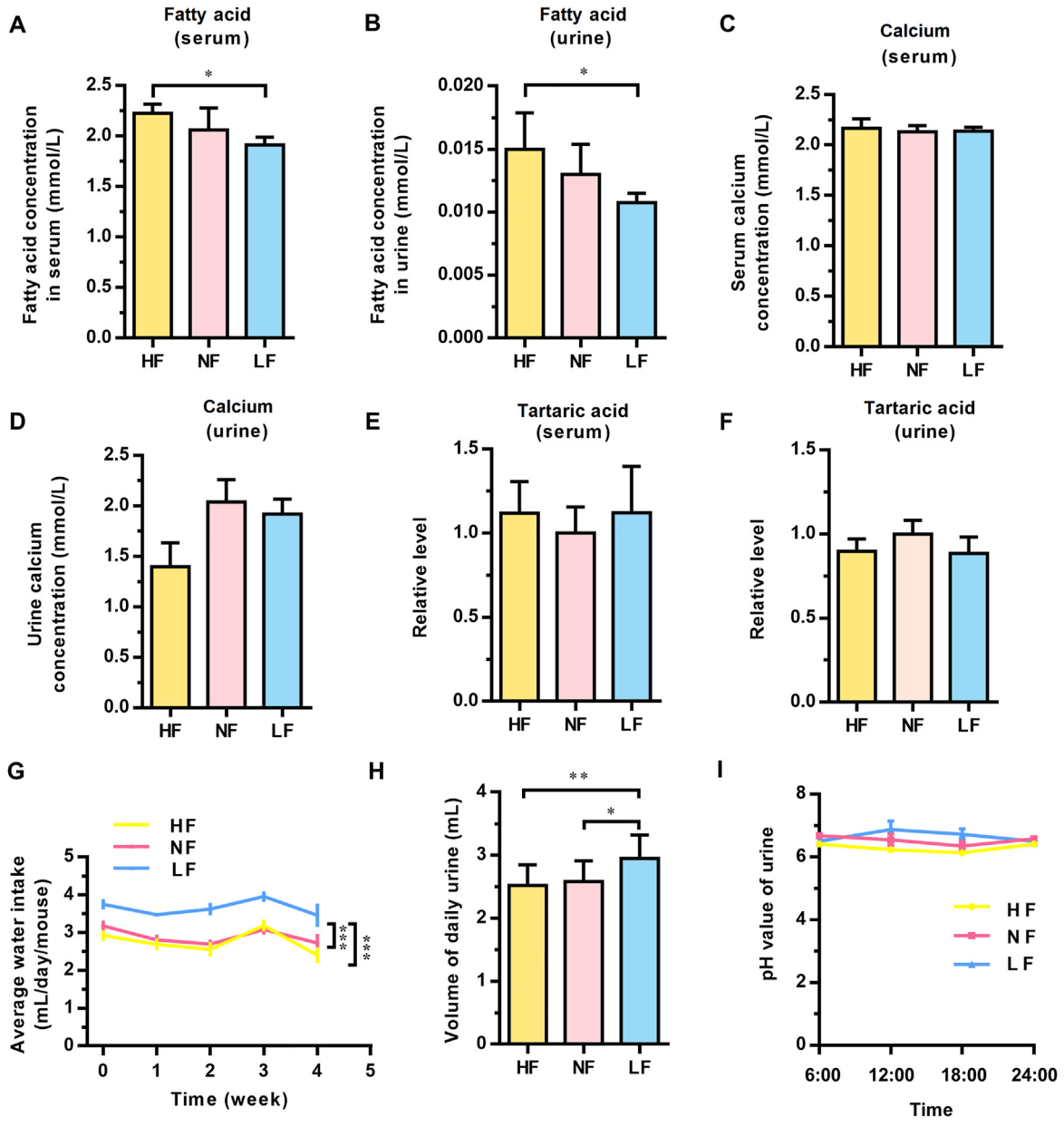

Figure 3 Shift in physicochemical properties did not account for the change in calculi morbidity. The relative levels of fatty acids in serum (A) and urine (B) after 4 weeks of dietary intervention. The relative levels of calcium in serum (C) and urine (D) after 4 weeks of dietary intervention. The relative levels of tartaric acid in serum (E) and urine (F) after 4 weeks of dietary intervention. (G) The daily water intake was measured every week. "0" represents the data from the acclimation period. (H) The relative urine volume of each mouse after 4 weeks of dietary intervention. (I) The urinary pH values at different time points in one day after 4 weeks of dietary intervention. HF, high-fat; NF, normal-fat; LF, low-fat. Data are presented as the mean ± SEM; $n = 4–6$. Significance was determined by the one-way ANOVA; $^{*}P < 0.05$, $^{**}P < 0.01$, $^{***}P < 0.001$.

result suggested that some biological alterations, rather than physicochemical changes, more likely influenced the formation of primary vesical calculi.

3.3. The gene expression profile of the bladder was partially changed in the different groups

From the results above, we realized that the traditional view, such as the volume of drinking water or pH of urine, could not explain the effect of dietary fat on the formation of primary vesical calculi. How does dietary fat affect the formation of vesical calculi? To elucidate the molecular mechanism of this process, bladder tissues were analyzed by RNA sequencing after 4 weeks of dietary intervention. The Venn diagram showed that 9 genes overlapped among the three gene sets: 94 (44 + 10 + 31 + 9) genes were differentially expressed between the NF and LF groups, 2313 (1214 + 1059 + 9 + 31) between the NF and HF groups, and 1762 (44 + 9 + 1059 + 650) between the HF and LF groups (Fig. 4A). The 9 genes that changed in the same direction were statistically clustered in a heat map (Fig. 4B).

Considering that calculi formation is an extracellular process, *Cxcl14*, which was the only gene that encodes excreted protein

among the 9 genes, was most likely to be responsible for the difference in calculi incidence among the groups. We examined the expression of *Cxcl14* in bladders in different groups through RT-qPCR, and the level of *Cxcl14* in the HF group was significantly increased compared with that in the NF and LF groups. We also examined the expression of the CXCL14 protein in bladders through Western blotting (Fig. 4C). Similar to the sequencing and RT-qPCR results, CXCL14 expression was significantly higher in the HF group than in the NF and LF groups (Fig. 4D). The immunofluorescence results also reveal that the protein level of CXCL14 in the bladder was significantly higher in the HF group than in the NF and LF groups (Fig. 4E).

3.4. Macrophage recruitment in the bladder was promoted in high-fat diet mice

After 4 weeks of intervention with different dietary fat contents, the integrity of the microstructure of the epithelia in the bladder mucosa layer was maintained in the HF group, while the NF and LF groups showed mild damage (Supporting Information Fig. S5A). Alizarin red staining showed that the HF group had the most calcium crystals in the bladder urothelium, significantly more than that in the NF and LF groups (Fig. S5B). The surface of the bladder urothelium in the NF and LF groups showed "spiculation-like" changes. Immunohistochemical staining of the

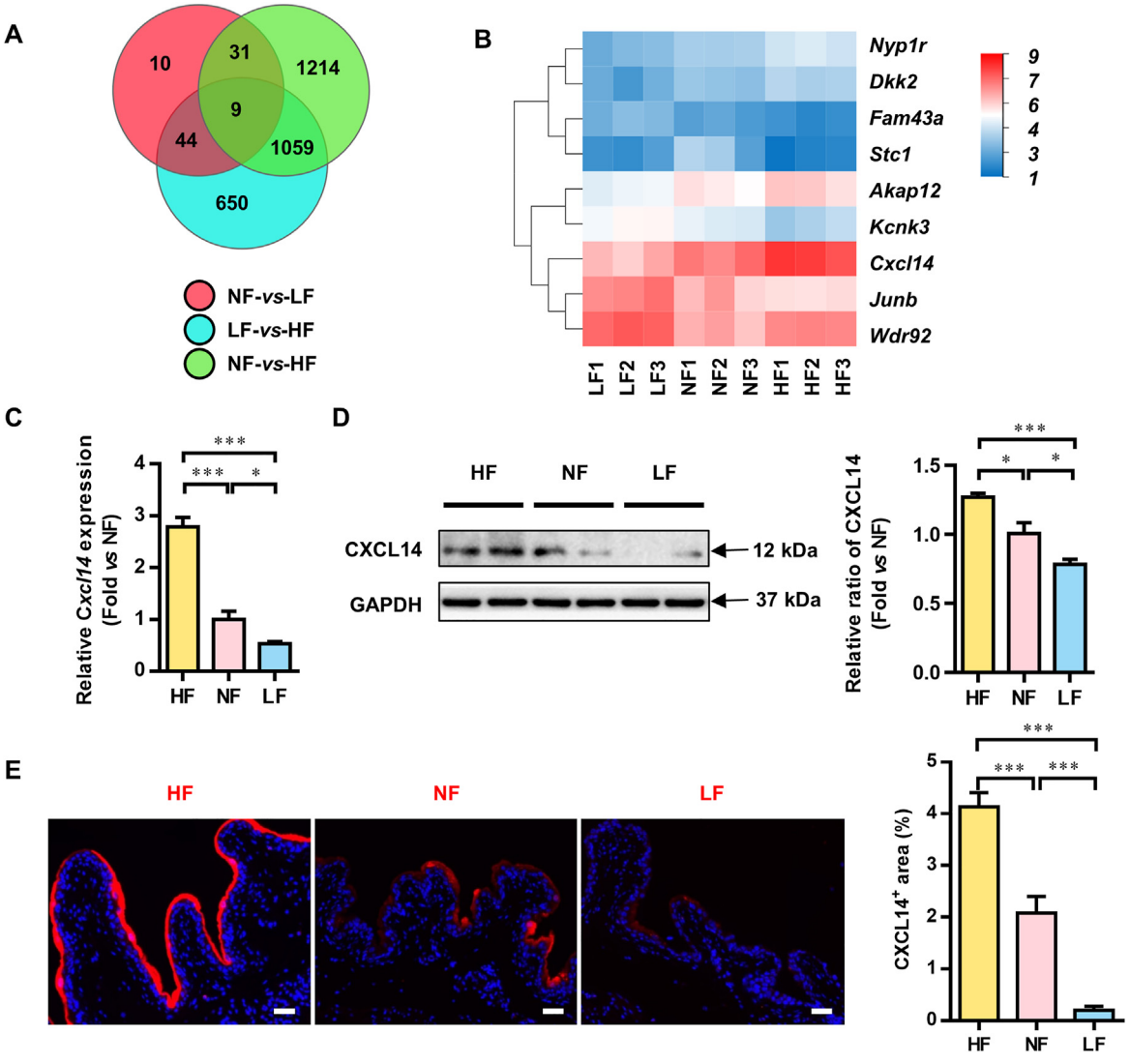

Figure 4 The gene expression profile of the bladder of mice after 4 weeks of different dietary fat content interventions. (A) The number of overlapping genes among the gene sets from bladder tissue after 4 weeks of dietary intervention. The screening criteria were $P < 0.05$ and more than twofold expression changes. (B) Relative expression of the 9 genes in the different groups after 4 weeks of dietary intervention. (C) mRNA expression of the C−X−C motif chemokine ligand 14 (*Cxcl14*) genes. (D) Representative Western blotting analysis and statistical results of CXCL14 protein expression in bladders from the HF, NF and LF groups after 4 weeks of dietary intervention. (E) Immunofluorescence staining and statistical analysis of CXCL14 in bladders after 4 weeks of dietary intervention. HF, high-fat; NF, normal-fat; LF, low-fat. α-kinase anchor protein 12 A, *Akap12*; C−X−C motif chemokine ligand 14, *Cxcl14*; dickkopf 2, *Dkk2*; neuropeptide Y(1) receptor, *Npy1r*; family with sequence similarity 43, member A, *Fam43a*; potassium channel subfamily K member 3, *Kcnk3*; recombinant Jun B proto oncogene, *Junb*; stanniocalcin-1, *Stc*1; WD repeat domain 92, Wdr92. Data are presented as the mean ± SEM; $n = 6$. Significance was determined by the one-way ANOVA; $^{*}P < 0.05$, $^{**}P < 0.01$, $^{***}P < 0.001$. Scale bar, 10 μm.

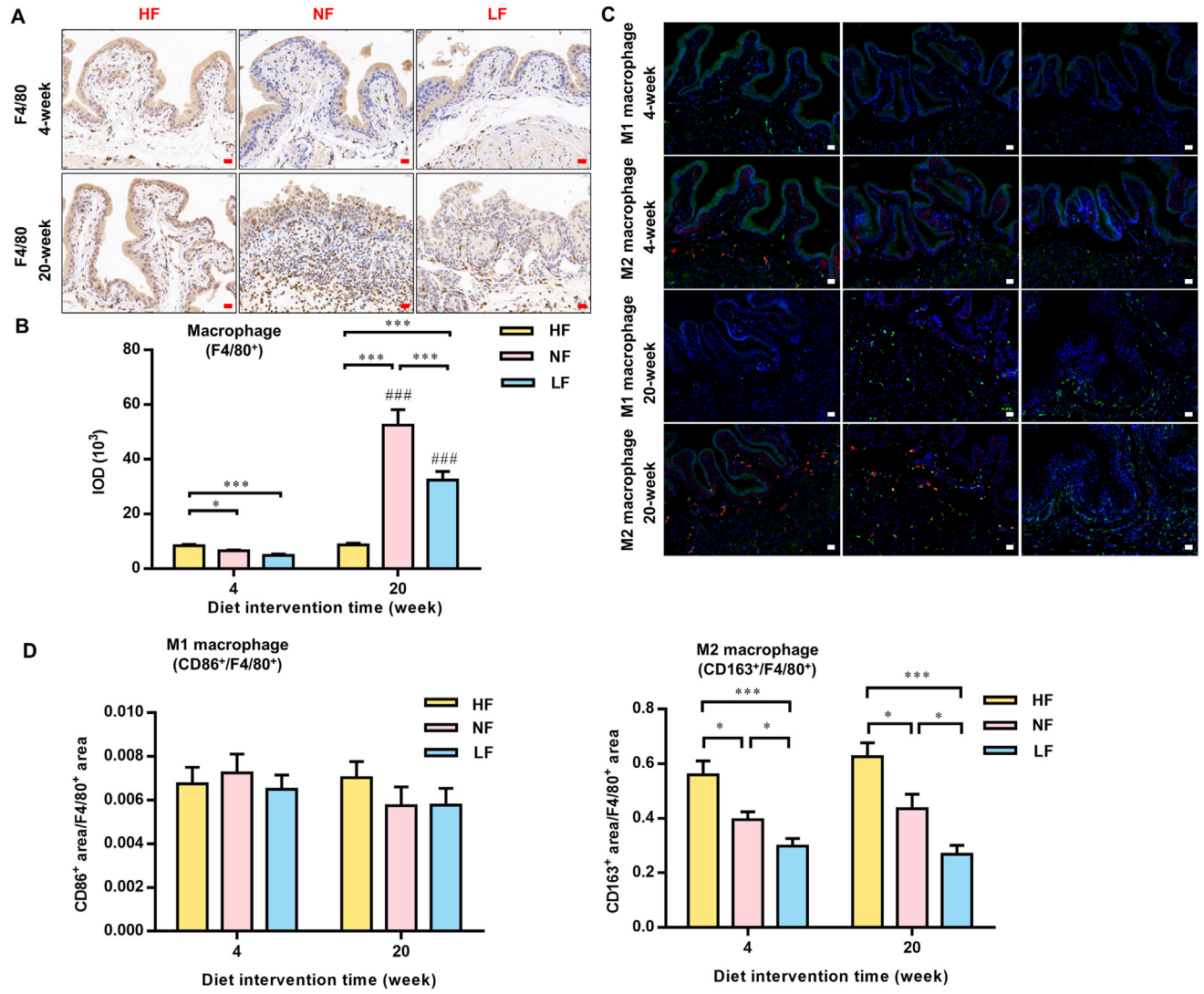

Figure 5 High-fat intake increased bladder macrophage infiltration and further promoted crystal absorption. (A) and (B) Immunohistochemical staining and statistical results of F4/80 of bladders after 4 weeks and 20 weeks of dietary intervention. (C) and (D) Immunofluorescence staining and statistical results of $CD86^+$ (red) and $F4/80^+$ (green) in the bladder (M1 macrophages were $CD86^+/F4/80^+$) and $CD163^+$ (red) and $F4/80^+$ (green) in the bladder (M2 macrophages were $CD163^+/F4/80^+$). HF, high-fat; NF, normal-fat; LF, low-fat. Data are presented as the mean ± SEM; $n = 6$. Significance was determined by the one-way ANOVA; $^*P < 0.05$, $^{***}P < 0.001$; $^{\#\#\#}P < 0.001$; compared with the same dietary pattern after a 4-week dietary intervention. Scale bar, 10 μm.

macrophage marker F4/80 showed that the macrophages in the HF group had a higher infiltration level and an obvious trend of aggregation in the bladder urothelium compared to those in the NF and LF groups when treated for four weeks. When the experiment continued, at 20 weeks, the developed vesical calculi induced a severe inflammatory response in the NF and LF groups, and the infiltration level became higher than that in the HF groups. Interestingly, even though there were larger vesical calculi in the LF groups than in the NF groups, the recruitment of macrophages was repressed in the LF group (Fig. 5A and B). Macrophages can be divided into "classic"/M1 and "alternative"/M2 subtypes, which play opposite roles in immune and inflammatory responses. Cereijo et al.[18] reported that CXCL14 secreted by brown adipocytes attracted alternatively polarized M2 macrophages and favored M2 polarization. The number of polarized M1 ($CD86^+/F4/80^+$) macrophages in the bladder shows no difference among these groups (Fig. 5C and D). However, the number of polarized M2 ($CD163^+/F4/80^+$) macrophages significantly increased in the HF group compared with the NF and LF groups (Fig. 5C and D).

3.5. *Fatty acid supplementation increased the expression of CXCL14 in HCV-29 cells*

Through animal experiments, we found that a high-fat diet significantly increased the levels of fatty acids in serum and urine. Next, to test whether fatty acids were the effector compounds in this process, we treated HCV-29 cells with different doses of fatty acid for 24 h. The addition of trace fatty acids did not affect the pH values of the DMEM cell medium (Supporting Information Fig. S6). However, the amount of CXCL14 protein was significantly increased in the supernatant of HCV-29 cells treated with the mixture of fatty acids. The amount of CXCL14 protein showed an increasing trend with the concentration of palmitic acid and oleic acid (Fig. 6A). Supplementation with

fatty acids also significantly increased the *CXCL14* mRNA level (Fig. 6B) and CXCL14 protein level (Fig. 6C) in the cells. Since calculi are often accompanied by biomineralization, we also tested the expression of transcription factor for osteogenic differentiation gene runt-related transcription factor 2 (*RUNX2*). No difference of *RUNX2* expression was observed with D,L-choline tartrate treatment for 24 h in HCV-29 cells (Supporting Information Fig. S7).

Taken together, in the model mice with primary vesical calculi, budding crystals formed in the upper mucosal layer of the bladder. With sufficient fatty acids, the integrity of the upper mucosa of the bladder was maintained, and bladder epithelial cells secreted CXCL14. CXCL14 induced local macrophages to differentiate into the M2 type, which was more efficient for crystal clearance[19]. Under fatty acid-deficient conditions, a lack of macrophages caused the accumulation of crystals that grew into pathogenic calculi (Fig. 6D).

4. Discussion

Although the morbidity of primary vesical calculi, especially in children, has dramatically declined in recent decades in developed countries, many children in developing countries are still suffering from this disease[1,2,20]. Practically, the addition of cow milk, meat, or eggs to the infant diet was found to be effective for the prevention of primary vesical calculi[2]. However, the role of fat, which has a higher proportion than protein in milk, has not been clearly elucidated as affecting vesical calculi formation[21]. In the current

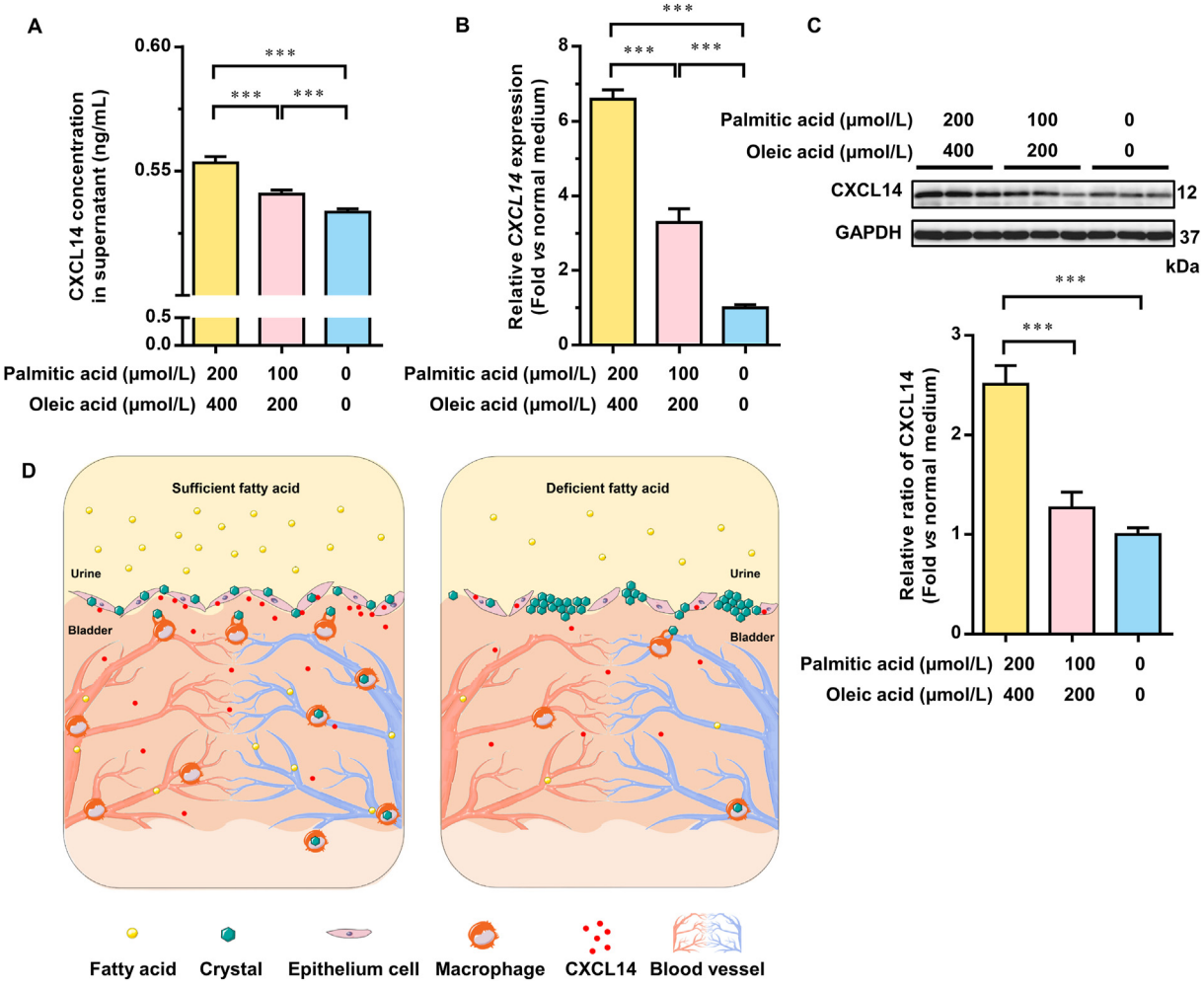

Figure 6 Sufficient fatty acids protected the bladder from calculi by promoting CXCL14 secretion by bladder epithelial cells. (A) The protein level of C−X−C motif chemokine ligand 14 (CXCL14) in the supernatant of HCV-29 cells treated with mixed fatty acids for 24 h was detected by enzyme-linked immunosorbent assay. (B) mRNA expression of the *CXCL14* gene in HCV-29 cells treated with mixed fatty acids for 24 h. (C) Representative Western blotting and statistical analysis results of CXCL14 protein expression in HCV-29 cells treated with different doses of fatty acids for 24 h. (D) Schematic diagram representing the effect of fatty acids on calculi formation in the bladder. In the model mice with primary vesical calculi, budding crystals formed in the upper mucosal layer of the bladder. With sufficient fatty acids, the integrity of the upper mucosa was maintained. Bladder epithelial cells secrete CXCL14. CXCL14 induced local macrophages to differentiate into the M2 type, which increased further macrophage recruitment, and then the crystals formed on the surface of epithelial cells in the bladder could be cleared by macrophages. Under fatty acid-deficient conditions, a lack of macrophages caused the accumulation of crystals that grew into pathogenic calculi. For the cell experiments, at least three independent experiments were performed. Data are presented as the mean ± SEM; $n = 6$. Significance was determined by the one-way ANOVA; ***$P < 0.001$.

study, we emphasized the importance of dietary fat for bladder health and expanded our understanding of bladder physiology and primary vesical calculi pathogenesis.

A novel primary vesical calculus mouse model with D,L-choline tartrate was established in this study (Figs. 1 and 2). Primary vesical calculi, formed in the bladder without injury to the upper urinary tract, have obvious advantages for investigating the early stage of the pathological process and mechanism of vesical calculi formation, including the formation, attachment, and clearance of crystal nuclei around bladder epithelia. The relatively simple composition of the vesical calculi (Fig. 1E and F) enhanced the repeatability of the experimental results. There was no difference in the concentration of calcium or tartaric acid among the three groups in either serum (Fig. 3C and E) or urine (Fig. 3D and F). In addition, we observed an increased daily water intake and higher urine pH in the LF group than in the HF group. These results were not completely consistent with previous research showing that drinking a large amount of water and lower urine pH can promote urination, which is beneficial for preventing urinary stones[22]. The above results revealed that changes in the physicochemical properties, including calcium or tartaric acid absorption, daily water intake, and alteration of urine pH, could not account for the diminished calculi formation in the HF group. Thus, it is more likely that some biological changes in the bladder influenced the formation of primary vesical calculi.

Fatty acids significantly ameliorated intestinal epithelial injury and helped protect the intestinal mucosal barrier function integrity induced by intestinal damage[23,24]. In our study, higher fatty acid levels in serum and urine were found in the HF group (Fig. 3A and B), and more integrated epithelia were observed in the bladder tissue in the HF group than in the normal- and low-fat diet groups, which may benefit from the protective effect of fatty acids on the epithelia of bladder tissue.

Macrophages play an essential role in urolithiasis[25], including the clearance of small crystals, regulation of inflammatory reactions, and repair of local tissues. It was reported that in a high-fat diet mouse model, fatty acids increased the number of lung macrophages[26]. In this study, transcriptome analysis indicated that macrophage recruitment was the main mechanism for preventing vesical calculi under a high-fat diet. Among the high-, normal- and low-fat diets, the low-fat diet induced the most remarkable changes in the transcriptome (Fig. 4A), which also resulted in the most significant changes in vesical calculus formation (Fig. 2D−F). Therefore, the most critical gene was among the 9 genes that were differentially transcribed in all three groups. The transcription pattern of 7 of those 9 genes changed in accordance with vesical calculi morbidity. Among the 7 genes, potassium channel subfamily K member 3 (*Kcnk3*) encodes a potassium channel expressed in adipocytes[27], but there are few adipocytes distributed in the bladder. Neuropeptide Y(1) receptor (*Npy1r*) encodes a G-protein coupled receptor that is mainly expressed in the nervous system[28]. Family with sequence similarity 43, member A (*Fam43a*) is a rarely studied gene with very low expression in the bladder. The remaining 4 genes, recombinant Jun B proto oncogene (*Junb*), α-kinase anchor protein 12 A (*Akap12*), dickkopf 2 (*Dkk2*), and *Cxcl14*, were reported to be related to macrophage activation[29] or differentiation[18,30,31], which indicated the important role of macrophages in preventing fat-related vesical calculi. *Akap12*, *Dkk2*, and *Cxcl14* are responsible for the differentiation of macrophages into the M2 type, which was reported to be more efficient than the M1 type in suppressing crystallization in the kidney[19].

5. Conclusions

In this study, a novel primary vesical calculus mouse model was established. Our research reveals that a high-fat diet could significantly decrease the morbidity of primary vesical calculi, emphasizing that fat was one of the main contributors to the prevention of primary vesical calculi and that macrophage recruitment was responsible for the suppression of urolithiasis. These results provide new knowledge regarding the relationship between diet and vesical calculi, which provides a different approach for preventing urolithiasis. In our previously published study, a high-fat diet rescued the premature aging phenotype and extended the shortened lifespan induced by SIRT6 deficiency[32]. This study provides a further theoretical basis for use of a high-fat diet against malnutrition-related diseases.

Acknowledgments

This work was supported by grants from the National Natural Science Foundation of China (81974503 and 81871095), the National Key R&D Program of China (2018YFC2000304), the Key International S&T Cooperation Program of China (2016YFE0113700), the European Union's Horizon 2020 Research and Innovation Program (633589), the Natural Science Foundation of Beijing, China (7202096), and the Tsinghua University independent research program (7191007, China).

Author contributions

The authors' responsibilities were as follows: Huiling Chen, Kaiqiang Hu and Zhao Wang conceived the study; Huiling Chen, Kaiqiang Hu and Yaru Liang designed the experiments; Huiling Chen, Yuqi Gao, Chenye Zeng and Xiaojin Shi performed most of the experiments; Yuemiao Yin, Liyuan Li and Kang Xu performed animal feeding, dissection, and tissue staining; Ying Qiu conducted staining analyses; Yi Qiao participated in literature research and provided clinical perspective on this project; Qingfei Liu and Zhao Wang contributed to the discussion and data interpretation; Huiling Chen and Kaiqiang Hu wrote the manuscript. All authors have read and agreed to the published version of the manuscript.

Conflicts of interest

The authors declare that they have no conflicts of interest.

Appendix A. Supporting information

Supporting data to this article can be found online at https://doi.org/10.1016/j.apsb.2021.08.001.

References

1. Soliman NA, Rizvi SAH. Endemic bladder calculi in children. *Pediatr Nephrol* 2017;**32**:1489−99.
2. Halstead SB. Epidemiology of bladder stone of children: precipitating events. *Urolithiasis* 2016;**44**:101−8.
3. Xu CF, Gao XL, Du YX, Ren ST. The rapid establishment and implications of a melamine-induced standardized bladder stone model in mice. *Food Chem Toxicol* 2011;**49**:3013−7.

4. Liu L, Luo M, Xiong X, Zhao L, Wang X, Ni L, et al. Peptidome profiles in melamine diet-induced bladder stones in C57BL/6 mice. *Toxicol Appl Pharmacol* 2019;**385**:114786.
5. Yuruk E, Tuken M, Sahin C, Kaptanagasi AO, Basak K, Aykan S, et al. The protective effects of an herbal agent tutukon on ethylene glycol and zinc disk induced urolithiasis model in a rat model. *Urolithiasis* 2016;**44**:501−7.
6. Wang Z, Bai Y, Wang J, Wang J. The preventive and therapeutic effects of alpha-lipoic acid on ethylene glycol-induced calcium oxalate deposition in rats. *Int Urol Nephrol* 2020;**52**:1227−34.
7. Ball GL, McLellan CJ, Bhat VS. Toxicological review and oral risk assessment of terephthalic acid (TPA) and its esters: a category approach. *Crit Rev Toxicol* 2012;**42**:28−67.
8. Li J, Wang W, An H, Wang F, Rexiati M, Wang Y. *In vitro* culture of rat hair follicle stem cells on rabbit bladder acellular matrix. *Springerplus* 2016;**5**:1461.
9. Melnick RL, Boorman GA, Haseman JK, Montali RJ, Huff J. Urolithiasis and bladder carcinogenicity of melamine in rodents. *Toxicol Appl Pharmacol* 1984;**72**:292−303.
10. Rofe AM, Bais R, Conyers RA. The effect of dietary refined sugars and sugar alcohols on renal calcium oxalate deposition in ethylene glycol-treated rats. *Food Chem Toxicol* 1986;**24**:397−403.
11. Kodama S, Yamamoto A, Matsunaga A, Hayakawa K. Direct chiral resolution of tartaric acid in food products by ligand exchange capillary electrophoresis using copper(II)-D-quinic acid as a chiral selector. *J Chromatogr A* 2001;**932**:139−43.
12. Newland MC, Reile PA, Sartin EA, Hart M, Craig-Schmidt MC, Mandel I, et al. Urolithiasis in rats consuming a dl bitartrate form of choline in a purified diet. *Comp Med* 2005;**55**:354−67.
13. Kleinguetl C, Williams Jr JC, Ibrahim SA, Daudon M, Bird ET, El Tayeb MM. Calcium tartrate tetrahydrate, case report of a novel human kidney stone. *J Endourol Case Rep* 2017;**3**:192−5.
14. Okada A, Yasui T, Fujii Y, Niimi K, Hamamoto S, Hirose M, et al. Renal macrophage migration and crystal phagocytosis *via* inflammatory-related gene expression during kidney stone formation and elimination in mice: detection by association analysis of stone-related gene expression and microstructural observation. *J Bone Miner Res* 2010;**25**:2701−11.
15. Taguchi K, Hamamoto S, Okada A, Unno R, Kamisawa H, Naiki T, et al. Genome-wide gene expression profiling of Randall's plaques in calcium oxalate stone formers. *J Am Soc Nephrol* 2017;**28**:333−47.
16. Taguchi K, Okada A, Hamamoto S, Iwatsuki S, Naiki T, Ando R, et al. Proinflammatory and metabolic changes facilitate renal crystal deposition in an obese mouse model of metabolic syndrome. *J Urol* 2015;**194**:1787−96.
17. Li X, Zhou L, Zhang Z, Liu Y, Liu J, Zhang C. IL-27 alleviates airway remodeling in a mouse model of asthma *via* PI3K/Akt pathway. *Exp Lung Res* 2020;**46**:98−108.
18. Cereijo R, Gavalda-Navarro A, Cairo M, Quesada-Lopez T, Villarroya J, Moron-Ros S, et al. CXCL14, a brown adipokine that mediates brown-fat-to-macrophage communication in thermogenic adaptation. *Cell Metab* 2018;**28**:750−763 e6.
19. Taguchi K, Okada A, Hamamoto S, Unno R, Moritoki Y, Ando R, et al. M1/M2-macrophage phenotypes regulate renal calcium oxalate crystal development. *Sci Rep* 2016;**6**:35167.
20. Ellis A. Histroy of bladder calculi. *J R Soc Med* 1979;**72**:248−51.
21. Andreas NJ, Kampmann B, Mehring Le-Doare K. Human breast milk: a review on its composition and bioactivity. *Early Hum Dev* 2015;**91**:629−35.
22. Bao Y, Tu X, Wei Q. Water for preventing urinary stones. *Cochrane Database Syst Rev* 2020;**2**:CD004292.
23. Xiao G, Yuan F, Geng Y, Qiu X, Liu Z, Lu J, et al. Eicosapentaenoic acid enhances heatstroke-impaired intestinal epithelial barrier function in rats. *Shock* 2015;**44**:348−56.
24. Xiao K, Liu C, Qin Q, Zhang Y, Wang X, Zhang J, et al. EPA and DHA attenuate deoxynivalenol-induced intestinal porcine epithelial cell injury and protect barrier function integrity by inhibiting necroptosis signaling pathway. *FASEB J* 2020;**34**:2483−96.
25. Kusmartsev S, Dominguez-Gutierrez PR, Canales BK, Bird VG, Vieweg J, Khan SR. Calcium oxalate stone fragment and crystal phagocytosis by human macrophages. *J Urol* 2016;**195**:1143−51.
26. Tashiro H, Takahashi K, Sadamatsu H, Kato G, Kurata K, Kimura S, et al. Saturated fatty acid increases lung macrophages and augments house dust mite-induced airway inflammation in mice fed with high-fat diet. *Inflammation* 2017;**40**:1072−86.
27. Chen Y, Zeng X, Huang X, Serag S, Woolf CJ, Spiegelman BM. Crosstalk between KCNK3-mediated ion current and adrenergic signaling regulates adipose thermogenesis and obesity. *Cell* 2017;**171**:836−48. e13.
28. Wang L, Rao F, Zhang K, Mahata M, Rodriguez-Flores JL, Fung MM, et al. Neuropeptide Y_1 receptor NPY1R discovery of naturally occurring human genetic variants governing gene expression in cella as well as pleiotropic effects on autonomic activity and blood pressure *in vivo*. *J Am Coll Cardiol* 2009;**54**:944−54.
29. Fontana MF, Baccarella A, Pancholi N, Pufall MA, Herbert DR, Kim CC. JUNB is a key transcriptional modulator of macrophage activation. *J Immunol* 2015;**194**:177−86.
30. Lin SL, Li B, Rao S, Yeo EJ, Hudson TE, Nowlin BT, et al. Macrophage Wnt7b is critical for kidney repair and regeneration. *Proc Natl Acad Sci U S A* 2010;**107**:4194−9.
31. Yang JM, Lee HS, Seo JH, Park JH, Gelman IH, Lo EH, et al. Structural environment built by AKAP12+ colon mesenchymal cells drives M2 macrophages during inflammation recovery. *Sci Rep* 2017;**7**:42723.
32. Li Z, Xu K, Guo Y, Ping L, Gao Y, Qiu Y, et al. A high-fat diet reverses metabolic disorders and premature aging by modulating insulin and IGF1 signaling in SIRT6 knockout mice. *Aging Cell* 2020;**19**:e13104.